Electrochemical and Solid-State Letters, **10** (6) H184-H185 (2007)
1099-0062/2007/10(6)/H184/2/$20.00 © The Electrochemical Society

Effect of Oxide on Trench Edge Defect Formation in Ion-Implanted Silicon

N. Burbure, N. G. Rudawski,[z] and K. S. Jones*

Department of Materials Science and Engineering, University of Florida, Gainesville, Florida 32611-6400, USA

An investigation of the defects that form near oxide-filled trenches during solid-phase epitaxy of amorphous silicon produced by ion implantation was conducted. It was observed that defects form near the trench edge after recrystallization. Defect formation resulted from pinning of the initial amorphous/crystalline interface at the trench edge and regrowth proceeded until triangular amorphous regions bound by the surface, trench, and (111) plane were formed. Regrowth of the triangular regions then proceeded along the [111] direction and was highly defective after recrystallization. Annealing of specimens with oxide-free trenches produced smaller defective regions compared to oxide-filled trenches.
 [DOI: 10.1149/1.2719597]

Manuscript submitted December 20, 2006; revised manuscript received February 7, 2007.
Available electronically March 28, 2007.

It has been known that stress from oxide (SiO_2) trench structures in ion-implanted silicon (Si) wafers can lead to the formation of defects near trench edges, which may cause device degradation or failure.[1-3] These defects typically form during high-temperature processing but may also occur during solid-phase epitaxy (SPE) of amorphous (α) Si. It is known that SPE in bulk Si can lead to the formation of {111} stacking faults as well as other secondary defects.[4] More relevantly, regrowth of two-dimensional α-Si regions via simultaneous SPE of two orthogonal fronts with different crystal orientations in patterned wafers can produce defects near the mask-edge.[5-7] However, the formation of defects during SPE near trench structures is not well understood. In the case of high-dose arsenic (As) implantation well in excess of solubility, trench-edge defects were observed as a result of regrowth interface pinning during SPE.[8] Furthermore, As^+-implantation is known to cause secondary defect formation at the projected range of implantation, and it is unclear whether the implanted species affects trench-edge defect formation.[9,10] Another explanation for trench-edge defects is the migration of point defects to regions of high stress generated by patterned structures, but this not thought to be related to SPE.[11] Thus, the goal of this study is to investigate the formation of trench-edge defects during SPE in Si wafers amorphized by Si^+ implantation.

For this study, 300 mm (001) wafers were patterned with SiO_2-filled trenches ~400 nm deep. After patterning, the wafers were implanted with Si^+ at energies of 10–80 keV and doses of 1×10^{15} to 1×10^{16} cm^{-2}. This produced α-Si layer depths ranging from 20 to 160 nm. Anneals were performed at 700 or 950°C using rapid thermal annealing (RTA). All anneals were preceded by a 10 s soak at 600°C. Transmission electron microscopy (TEM) was used to image α-Si regrowth in the vicinity of trench edges. Both cross-sectional TEM (XTEM) and plan-view TEM (PTEM) were used for this study. Imaging was performed using weak-beam dark-field (WBDF) or on-axis bright-field (BF) conditions.

Two repeating structures were investigated. The first structure was comprised of SiO_2-filled trench lines ~3.7 μm wide and spaced ~12.5 μm apart, while the second structure contained Si squares ~0.6 μm wide surrounded by a SiO_2-filled trench. Line and square structures produced very similar results in this study, and for clarity only line structures are presented. Figure 1 presents TEM micrographs showing the formation and location of defects for samples implanted with Si^+ at 40 keV to a dose of 1×10^{15} cm^{-2} and annealed at 950°C for 5 s using RTA. The WBDF XTEM micrograph of a line structure shown in Fig. 1a revealed that the defects nucleate along the Si/SiO_2 interface at the original α/crystalline interface and extend up to the surface, forming a triangular region of defective Si. WBDF PTEM of the completely regrown line and square structures confirmed the location of the defective Si relative to the trench edge, as shown in Fig. 1b.

Figure 2 shows the evolution of the defective Si regrowth using BF XTEM images of line structures. Figure 2a displays the as-implanted state, while Fig. 2b displays an image after partial completion of SPE following a 700°C spike RTA treatment. As shown in Fig. 2b, a triangular region of α-Si bound by the surface, trench edge, and α/crystalline interface remains. The angle of the α/crystalline interface normal is ~54° to [001], indicating it is the (111) plane. Thus, the incomplete recrystallization is possibly due to slower regrowth along [111] as well as the regrowth front being pinned at the interface between the initial α/crystalline interface and SiO_2.[12] Slower regrowth has also been attributed to recoiled oxygen (O) resulting from ion implantation.[13] A related study of partially recrystallized layers along trench edges determined that recoils could not be responsible for retarded SPE because the lateral straggle of the O does not overlay with the entire triangular region.[8] After performing RTA at 950°C for 5 s, the original triangular α-Si region recrystallized into highly defective Si, as shown in the BF XTEM image shown in Fig. 2c. This is consistent with observations of SPE for (111) substrate orientation, which typically contains a high concentration of stacking faults and microtwins.[4] Defects associated with growth in this direction were previously observed to form at angles to the (111) plane. However, in the case of the trench edge, defects appear to run parallel to the (111) plane and this discrepancy is not fully understood. Furthermore, the initial stages of defect formation were observed prior to completion of SPE and thus condensation of point defects is not believed to be a factor in trench-edge defect formation.

To gain a better understanding of the effect of the SiO_2-filled trench on the formation of this defect, SiO_2-free samples were analyzed. A specimen implanted with Si^+ at energies of 20 and 80 keV with doses of 1×10^{15} cm^{-2} was etched with hydrofluoric acid for 20 min to remove SiO_2 from the trenches. The sample was then annealed at 700°C for 1 min using RTA. Figures 3a and b present

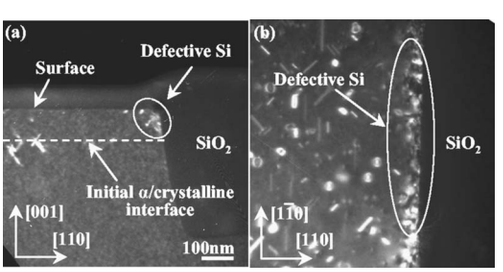

Figure 1. WBDF (a) XTEM and (b) PTEM images of a line structure implanted with Si^+ at 40 keV with a dose of 1×10^{15} cm^{-2} after annealing at 950°C for 5 s using RTA.

* Electrochemical Society Active Member.
[z] E-mail: ngr@ufl.edu

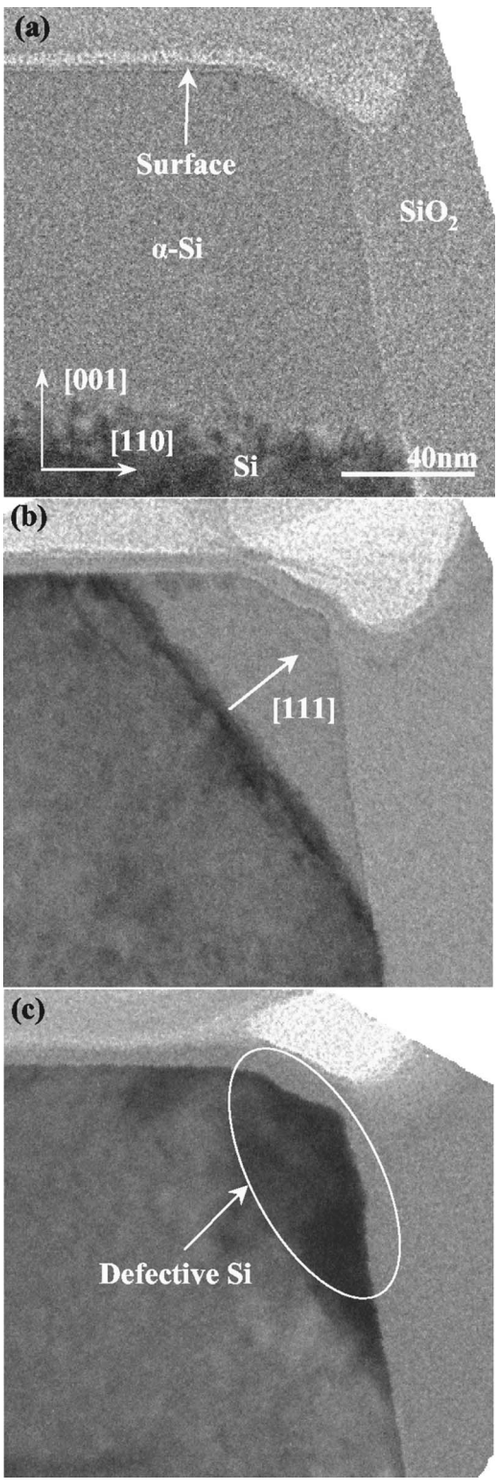

Figure 2. BF XTEM images of lines structures implanted with Si^+ at 40 keV with a dose of 1×10^{15} cm^{-2} (a) in the as-implanted state, (b) after 700°C spike RTA treatment, and (c) after RTA at 950°C for 5 s.

BF XTEM images of line structures annealed with and without SiO_2, respectively. In the sample possessing SiO_2-filled trenches, trench-edge defects nucleated near the original α/crystalline interface while in the SiO_2-free specimens, the defect nucleation was delayed until ~40 nm of regrowth occurred. The delay in defect formation was presumably due to easier recrystallization near a SiO_2-free trench relative to a SiO_2-filled trench, as no rearrangement of Si–O bonds need occur at a free surface. With further annealing, substantial SiO_2 grows in the trenches and defect nucleation begins. Thus, the presence of SiO_2 along the trench edges clearly influences defect formation. Furthermore, because recoiled O was present in both SiO_2-filled and SiO_2-free specimens, it follows that recoiled O was not a primary cause of defect formation. Finally, stress can influence the shape of a regrowing α/crystalline interface and it is worthwhile to consider this as stress from trench structures can be significant.[14,15] However, because both SiO_2-filled and SiO_2-free trench structures exhibited similar regrowth interfaces, the observations are likely not stress-related.

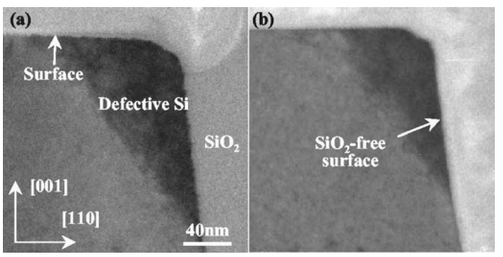

Figure 3. BF XTEM images of line structures implanted with Si^+ at energies of 20 and 80 keV with doses of 1×10^{15} cm^{-2} after annealing using RTA at 700°C for 1 min with (a) SiO_2-filled trenches and (b) SiO_2-free trenches.

Trench-edge defects were observed during regrowth of amorphous silicon in both line and square structures. It was determined that the trench structure affects solid-phase epitaxy by pinning the regrowth front at the oxide-filled trench edge. The regrowth front that results from partial recrystallization corresponds to the (111) plane with complete recrystallization proceeding along [111] and resulting in the formation of defects along the trench edge. Furthermore, while trench-edge defects were observed for all implantation energies and doses, the removal of oxide from the trenches prior to annealing delayed defect formation substantially. Thus, defect formation is strongly influenced by the presence of oxide during annealing, with point defect condensation and recoiled oxygen not believed to be very significant factors. However, further studies are required to fully understand additional factors contributing to trench-edge defect formation.

Acknowledgments

The authors acknowledge the Intel Corporation for funding this research.

University of Florida assisted in meeting the publication costs of this article.

References

1. P. M. Fahey, S. R. Mader, S. R. Stiffler, R. L. Mohler, J. D. Mis, and J. A. Slinkman, *IBM J. Res. Dev.*, **36**, 158 (1992).
2. S. M. Hu, *J. Appl. Phys.*, **67**, 1092 (1990).
3. D. Chidambarrao, J. P. Peng, and G. R. Srinivasan, *J. Appl. Phys.*, **70**, 4816 (1991).
4. K. S. Jones, S. Prussin, and E. R. Weber, *Appl. Phys. A*, **45**, 1 (1988).
5. H. Cerva and K.-H. Kusters, *J. Appl. Phys.*, **66**, 4723 (1989).
6. H. Cerva and W. Bergholz, *J. Electrochem. Soc.*, **140**, 780 (1993).
7. H. Cerva, *Defect Diffus. Forum*, **148**, 103 (1997).
8. G. Fuse, H. Iwasaki, and M. Onoda, *Appl. Phys. Lett.*, **59**, 2400 (1991).
9. A. Armigliato and A. Parisini, *J. Mater. Res.*, **6**, 1701 (1991).
10. S. N. Hsu and L. J. Chen, *Appl. Phys. Lett.*, **55**, 2304 (1989).
11. S. M. Hu, *J. Appl. Phys.*, **70**, R53 (1991).
12. L. Csepregi, E. F. Kennedy, and J. W. Mayer, *J. Appl. Phys.*, **49**, 3906 (1978).
13. E. F. Kennedy, L. Csepregi, J. W. Mayer, and T. W. Sigmon, *J. Appl. Phys.*, **48**, 4241 (1977).
14. N. G. Rudawski, K. N. Siebein, and K. S. Jones, *Appl. Phys. Lett.*, **89**, 082107 (2006).
15. C. R. Olson, E. Kuryliw, B. E. Jones, and K. S. Jones, *J. Vac. Sci. Technol. B*, **24**, 446 (2006).